UC Berkeley
UC Berkeley Previously Published Works

Title

The Influence of Ocean Coupling on Simulated and Projected Tropical Cyclone Precipitation in the HighResMIP–PRIMAVERA Simulations

Permalink

https://escholarship.org/uc/item/5fr1c492

Journal

Geophysical Research Letters, 48(20)

ISSN

0094-8276

Authors

Huang, Huanping
Patricola, Christina M
Collins, William D

Publication Date

2021-10-28

DOI

10.1029/2021gl094801

Copyright Information

Peer reviewed

Geophysical Research Letters®

Key Points:
- Ocean coupling generally leads to decreased tropical cyclone (TC) precipitation over both ocean and land
- Large-scale sea surface temperature biases and TC cold wakes, key facets of ocean coupling, drive the precipitation decline
- Projected future TC precipitation increases in most regions, however the magnitude can vary by a factor of three depending on ocean coupling

The Influence of Ocean Coupling on Simulated and Projected Tropical Cyclone Precipitation in the HighResMIP–PRIMAVERA Simulations

Huanping Huang[1] , **Christina M. Patricola[2,1]** , and **William D. Collins[1,3]**

[1]Climate and Ecosystem Sciences Division, Lawrence Berkeley National Laboratory, Berkeley, CA, USA, [2]Department of Geological and Atmospheric Sciences, Iowa State University, Ames, IA, USA, [3]Department of Earth and Planetary Science, University of California, Berkeley, Berkeley, CA, USA

Abstract This study aims to quantify the impacts of atmosphere–ocean coupling on simulated and projected tropical cyclone (TC) precipitation globally. We used global climate model (GCM) simulations over 1950–2050 from the High Resolution Model Intercomparison Project (HighResMIP) and compared its fully coupled atmosphere–ocean GCMs (AOGCMs) with atmosphere-only GCMs (AGCMs). We find that ocean coupling generally leads to decreased TC precipitation over ocean and land. Large-scale sea surface temperature (SST) biases are critical drivers of the precipitation difference, with secondary contributions from local TC–ocean feedbacks via SST cold wakes. The two driving factors, attributed to ocean coupling in the AOGCMs, influence TC precipitation in association with decreased TC intensity and specific humidity. The AOGCMs and AGCMs consistently project TC precipitation increases in 2015–2050 relative to 1950–2014 over ocean for all basins, and for landfalling TCs in the North Atlantic and western North Pacific.

Plain Language Summary Global climate models (GCMs) are important tools to simulate and project tropical cyclones (TCs) and associated precipitation. Yet there are large uncertainties in simulated TC precipitation, with atmosphere–ocean coupling in GCMs as a major source of uncertainty. In this study, we assess the impacts of ocean coupling on the representation and projection of TC precipitation. We find that the fully coupled atmosphere–ocean GCM simulations generally produce lower TC precipitation than the atmosphere-only GCM simulations (i.e., sea surface temperatures or SSTs prescribed from observations). The precipitation decrease is associated with large-scale SST underestimations and local TC–ocean interactions via SST cooling, common features in the GCM simulations with active atmosphere–ocean coupling. The two features influence TC precipitation by reducing TC intensity and specific humidity. During the period 2015–2050, TC precipitation is predicted to increase in most TC basins by both the fully coupled and atmosphere-only GCM simulations. However, the magnitude can vary by a factor of three depending on ocean coupling. Further research is needed to better understand and characterize the physical mechanisms governing the accurate representations of SSTs, TCs, and TC precipitation.

1. Introduction

Heavy precipitation and associated floods from tropical cyclones (TCs) have caused enormous damages to the economy and human health (Bell et al., 2018; Rappaport, 2014; Rappaport & Blanchard, 2016). Globally, TCs have resulted in US$23 billion of economic damages (adjusted to current value) and more than 9,500 fatalities per year over the past half a century (CRED, 2021), with excessive precipitation as one of the leading causes (Bakkensen et al., 2018; Bell et al., 2018). Among the 2,544 lives in the US claimed by Atlantic TCs over 1963–2012, about a quarter of the fatalities was attributed to TC precipitation (TCP)-induced floods and mudslides (Rappaport, 2014). Moreover, extreme precipitation (>750 mm) from Hurricane Harvey in 2017 caused unprecedented flooding over the greater Houston area, making the hurricane one of the costliest disasters (US$131 billion) in US history (NOAA National Centers for Environmental Information, 2021). Future climate change may double the economic damages of TCs by 2100 primarily through increased TC intensity, storm surge, and precipitation rate (Knutson et al., 2020; Mendelsohn et al., 2012; Patricola & Wehner, 2018). Therefore, it is imperative to accurately predict TCP and assess the risk with changing TCP.

Global climate models (GCMs), especially high resolution models (50 km and higher), are important tools to simulate and project TCs (Haarsma et al., 2016; Li & Sriver, 2018; Walsh et al., 2016; Wehner et al., 2015), as well as TC interactions with the climate system (Scoccimarro et al., 2020). But there exist large uncertainties in simulated TCs and associated precipitation, which are rooted in model physics, resolution, and experimental design (Hasegawa & Emori, 2007; Li & Sriver, 2018, 2019; Roberts et al., 2020a, 2020b; Zhang, Villarini, et al., 2021). In particular, atmosphere–ocean interactions in GCMs are a major source of uncertainty (Li & Sriver, 2018, 2019; Roberts et al., 2020b). Active atmosphere–ocean interactions, as observed in the real world and simulated by coupled atmosphere–ocean GCMs (AOGCMs), are crucial in correctly representing TC intensity, duration, and precipitation (Li & Sriver, 2018; Ma et al., 2020; Scoccimarro, Fogli, et al., 2017; Vincent, Lengaigne, Madec, et al., 2012; Zarzycki, 2016). Strong TC–ocean interactions usually cool sea surface temperatures (SSTs) along TC tracks due to strong winds of TCs (Vincent, Lengaigne, Madec, et al., 2012). The winds vertically mix and entrain surface warm water with lower-level colder water and enhance upwelling and ocean–atmosphere heat fluxes (Liu et al., 2011; Price, 1981; Vincent, Lengaigne, Madec, et al., 2012). The TC-induced SST cooling (cold wakes) is approximately 1°C on average and affects at least five radii of maximum wind (Vincent, Lengaigne, Madec, et al., 2012). As TCs obtain energy from the upper ocean, cold wakes generate a negative feedback to TCs via modulating enthalpy flux and regional atmospheric circulation (Karnauskas et al., 2021; Kushnir et al., 2002; Ma et al., 2020; Trenberth et al., 1998; Vincent, Lengaigne, Vialard, et al., 2012; Zarzycki, 2016). Therefore, they impose profound effects on TC characteristics and TCP (Karnauskas et al., 2021; Li & Sriver, 2019; Ma et al., 2020; Zarzycki, 2016). Cold wakes were found to decrease post-TC precipitation by 17% in the wakes (Ma et al., 2020). They can reduce the frequency of subsequent TCs by 10% and shorten the return period of Category 5 hurricanes by a factor of six across the North Atlantic (Karnauskas et al., 2021).

While AOGCMs are capable of simulating TC–ocean interactions, they produce large-scale SST biases (Richter, 2015; Richter & Tokinaga, 2020; Zhu et al., 2020) which can cause a substantial misrepresentation of TC activity (Hsu et al., 2019; Zhang, Murakami, et al., 2021). This deficiency leads to the common use of prescribed-SSTs with atmosphere-only GCMs (AGCMs), which by definition lack ocean coupling and therefore simulated cold wakes (Haarsma et al., 2016; Hsu et al., 2019; Roberts et al., 2020a; Vincent, Lengaigne, Madec, et al., 2012). The difference in ocean coupling between AGCMs and AOGCMs generates disparate TC activity and TCP (Hasegawa & Emori, 2007; Li & Sriver, 2018, 2019; Roberts et al., 2020b; Zarzycki, 2016). For example, Roberts et al. (2020b) found that for the North Atlantic TCs during 1979–2014, most AOGCMs underestimated its frequency by 16.7%–80% as compared to AGCMs. While AGCMs predicted future increases in TC frequency and Accumulated Cyclone Energy, AOGCMs estimated an increase only in Accumulated Cyclone Energy. Hasegawa and Emori (2007) reported the uncoupled MIROC 3.2 model simulated 6.6% more North Atlantic TCP than its coupled model with fixed anthropogenic forcing in 1900. After doubling CO_2 from its 1900 level, the uncoupled model predicted increased TCP (10.4%), but the coupled model yielded a negligible change (0.6%). Yet, the influence of ocean coupling on the representation and projection of TCP remains poorly characterized, especially with multi-model ensembles and state-of-the-art GCMs.

The High Resolution Model Intercomparison Project (HighResMIP; Haarsma et al., 2016) provides a unique opportunity to examine the impact of ocean coupling on simulated and projected TCP. HighResMIP conducted both AGCM and AOGCM experiments with the same set of GCMs, different horizontal resolutions (varying from 150 to 25 km), and time-varying external forcings spanning 1950–2050 (Haarsma et al., 2016). Its outputs have been used to investigate global TC activity with both AGCMs and AOGCMs (Roberts et al., 2020a, 2020b), as well as global land precipitation and TCP based on the AGCMs (Bador et al., 2020; Zhang, Villarini, et al., 2021). Nevertheless, assessing the effect of ocean coupling on TCP is still lacking. Therefore, we address the following questions: (a) How does the representation of TCP differ in the HighResMIP AGCM and AOGCM simulations? (b) What physical processes are responsible for any TCP differences? (c) How does ocean coupling affect projections of future TCP? We first compared the differences in simulated TCP over 1950–2014 between the AOGCMs and AGCMs in low- and high-resolutions, and evaluated their performance relative to observations. Then we quantified the impacts of two ocean coupling features (large-scale SST biases and local SST feedback to TCs) on simulated TCP. Lastly, we assessed projected changes in TCP during 2015–2050 (relative to 1950–2014) and associated uncertainties due to ocean

coupling. Given the length constraints of the paper, we focus on the findings for the Northern Hemisphere in the main text and present the results for the Southern Hemisphere in the Supporting Information S1.

2. Data and Methods

2.1. Climate Model Simulations

Climate model simulations are derived from the HighResMIP (Haarsma et al., 2016), one of the Model Intercomparison Projects endorsed by the Coupled Model Intercomparison Project Phase 6 (CMIP6). Table S1 in Supporting Information S1 describes four different GCMs used in this study, including CMCC-CM2 (Cherchi et al., 2019), CNRM-CM6.1 (Voldoire et al., 2019), EC-Earth3P (Haarsma et al., 2020), and HadGEM3-GC3.1 (Roberts et al., 2019). This multi-model ensemble was produced by the European Union Horizon 2020 project PRIMAVERA which follows the HighResMIP protocol at both a CMIP6 standard (~100 km) and a high (25–50 km) horizontal resolution (Roberts et al., 2020a). Note that the remaining two GCMs (ECMWF and MPI-M) in the PRIMAVERA were not included in this study because of incomplete data (e.g., SST) available in the archive. The modeling centers listed in Table S1 in Supporting Information S1 conducted both AGCM (uncoupled) and AOGCM (coupled) simulations spanning 1950–2050 which covers historical (1950–2014) and future (2015–2050) periods. Details about the simulation design are described in Haarsma et al. (2016) and Roberts et al. (2020a) and summarized in Text S1 in Supporting Information S1.

Simulated TC tracks and their lifecycle were identified using two feature-tracking algorithms, TempestExtremes (Ullrich & Zarzycki, 2017) and TRACK (Hodges et al., 2017). They can be accessed through the Centre for Environmental Data Analysis (Roberts 2019a, 2019b). While both algorithms use criteria for warm-core and lifetime, their primary feature-tracking variables are different (sea level pressure in TempestExtremes and relative vorticity in TRACK). Characteristics of the HighResMIP-based TC tracks were summarized in Roberts et al. (2020a, 2020b). While both trackers yield more TCs in the high-resolution simulations than the lower-resolution simulations, the TRACK algorithm generally detects more frequent TCs than the TempestExtremes in both resolutions (Roberts et al., 2020a, 2020b). For the sake of brevity, we only discuss the results based on the TRACK algorithm in Section 3, which was available for a greater number of models than the TempestExtremes tracks. The results from the TempestExtremes algorithm are described in Figures S4 and S5 in Supporting Information S1, and the findings based on the two algorithms are similar.

2.2. Tropical Cyclone and Precipitation Observations

To evaluate the performance of the GCMs, we compared the simulated TCP to observations from the Tropical Rainfall Measuring Mission (TRMM) data set which integrates precipitation estimates from satellites and rain gauge analyses (Huffman et al., 2007). The data set is chosen to validate the HighResMIP simulations because of its high temporal (three hourly in the 3B42 subset) and spatial resolutions ($0.25° \times 0.25°$) covering 50°N–50°S (Huffman et al., 2007; TRMM, 2011). Given the time length of TRMM data (1998 to present), we compared the HighResMIP historical simulations with TRMM over only their common 17-year period (1998–2014).

Observed TC tracks in the North Atlantic and eastern North Pacific basins are maintained by the National Oceanic and Atmospheric Administration (NOAA) National Hurricane Center's hurricane database (HURDAT2; Landsea & Franklin, 2013). TC tracks in the western North Pacific and North Indian basins are documented by the U.S. Navy's Joint Typhoon Warning Center (JTWC) best-track database (Chu et al., 2002). Boundaries of the four TC basins in the Northern Hemisphere are defined in Figure S1 in Supporting Information S1.

2.3. Analysis Methods

We computed and compared TCP during the TC season (May–November in the Northern Hemisphere and October–May in the Southern Hemisphere) in the AOGCM and AGCM simulations and the TRMM data set. Here TCP is defined as average precipitation rate within a 500 km radius of TC center (Knutson et al., 2020). We calculated the percent difference in TCP (ΔTCP) associated with ocean coupling as in Equation 1. To

uncover possible causes of the difference in simulated TCP over 1950–2014, we also analyzed basin-averaged SSTs and TC minimum sea level pressure (SLP) and near-surface specific humidity (HUSS) within a 500 km radius of TC position. Differences in SST, SLP, and HUSS between the AOGCMs and AGCMs were computed from Equations 2–4. These climate variables were derived from the GCM outputs at the 6 hourly frequency to match with TC time steps. In addition, we estimated the percent change in future TCP relative to the historical period 1950–2014 for each AOGCM/AGCM simulation (Equation 5).

$$\Delta\text{TCP} = 100 * \left(\text{TCP}_{\text{AOGCM}} - \text{TCP}_{\text{AGCM}}\right)/\text{TCP}_{\text{AGCM}} \tag{1}$$

$$\Delta\text{SLP} = \text{SLP}_{\text{AOGCM}} - \text{SLP}_{\text{AGCM}} \tag{2}$$

$$\Delta\text{HUSS} = 100 * \left(\text{HUSS}_{\text{AOGCM}} - \text{HUSS}_{\text{AGCM}}\right)/\text{HUSS}_{\text{AGCM}} \tag{3}$$

$$\text{SST bias} = \text{SST}_{\text{AOGCM}} - \text{SST}_{\text{AGCM}} \tag{4}$$

$$\text{Future change in TCP} = 100 * \left(\text{TCP}_{\text{GCM,2015-2050}} - \text{TCP}_{\text{GCM,1950-2014}}\right)/\text{TCP}_{\text{GCM,1950-2014}} \tag{5}$$

$$\delta\text{SST} = \text{SST}_{\text{GCM,post-TC}} - \text{SST}_{\text{GCM,pre-TC}} \tag{6}$$

To quantify TC–ocean interactions in the simulations, we calculated the amplitude of cold wakes δSST in each AOGCM or AGCM (Equation 6). It is defined as the difference between post-TC (1–4 days after TC passage) SST and pre-TC (3–10 days before TC passage) SST averaged over a 200 km radius around each TC position (Vincent, Lengaigne, Madec, et al., 2012). We note that not all modeling centers provide SSTs (derived from surface temperatures over ocean) in their data archive, but surface upwelling longwave radiation is provided. When SSTs were not available, we derived SSTs from longwave radiation using the Stefan-Boltzmann law. We find no significant difference in cold wakes whether quantified using SST or longwave radiation (not shown), as demonstrated by the GCMs (HadGEM3-GC3.1 and CMCC-CM2) that have both SSTs and surface upwelling longwave radiation available in their data archive.

3. Results and Discussion

3.1. Observed and Simulated Tropical Cyclone Precipitation

Simulated TCP during the historical period is relatively insensitive to model resolution, for the same AGCM or AOGCM, but the GCMs tend to underestimate TCP as compared to the TRMM observations. Taking the North Atlantic Ocean as an example, the high- and low-resolution AGCMs simulate a median TCP of 0.63 and 0.66 mm h^{-1}, respectively (Figure 1a). Their AOGCM counterparts yield a median TCP of 0.49 and 0.54 mm h^{-1}, respectively (Figure 1b). Like the medians, the 95% confidence intervals (CIs) of TCP in the high- and low-resolution simulations are very close. Nevertheless, all GCMs (including coupled and uncoupled) underestimate TCP as compared to the TRMM observations 1998–2014, especially heavy TCP events (Figures S2a and S2e in Supporting Information S1). For example, the uncoupled (coupled) HadGEM3-GC3.1-HM model simulates 24.7% (54.6%) less TCP than TRMM over the North Atlantic. Zhang et al. (2019), Zhang, Murakami et al. (2021), and Zhang, Villarini, et al. (2021) also reported underestimated TCP, as well as its low sensitivity to model resolution. The undersimulated TCP can be attributed to GCMs' limitation in simulating strong TCs, even with model resolutions as high as 25–50 km (Roberts et al., 2020a). Similar to our findings over the North Atlantic, most of the AGCMs and AOGCMs underperform in capturing observed TCP over other TC basins (Figures S2 and S3 in Supporting Information S1).

3.2. The Impacts of Ocean Coupling on Tropical Cyclone Precipitation

Ocean coupling generally leads to decreased TCP over ocean (Figures 1c–1f). In the North Atlantic Ocean, TCP is 7.9%–28.6% lower in the eight AOGCMs than in their corresponding AGCMs. The high-resolution four-member AOGCM ensemble produces 20.8% less TCP than the AGCM ensemble (95% CI: [-21.3%, −20.4%]). The TCP difference in the low-resolution ensemble is −16.5% (95% CI: [−17%, −16.1%]), indicating a low sensitivity of TCP difference to model resolution (Figure 1c). For other ocean basins, we find a similar contrast in TCP arising from ocean coupling (Figures 1d–1f). Specifically, relative to the high-resolution AGCM ensemble, the high-resolution AOGCM ensemble simulates a difference in TCP of −1.3% (95% CI:
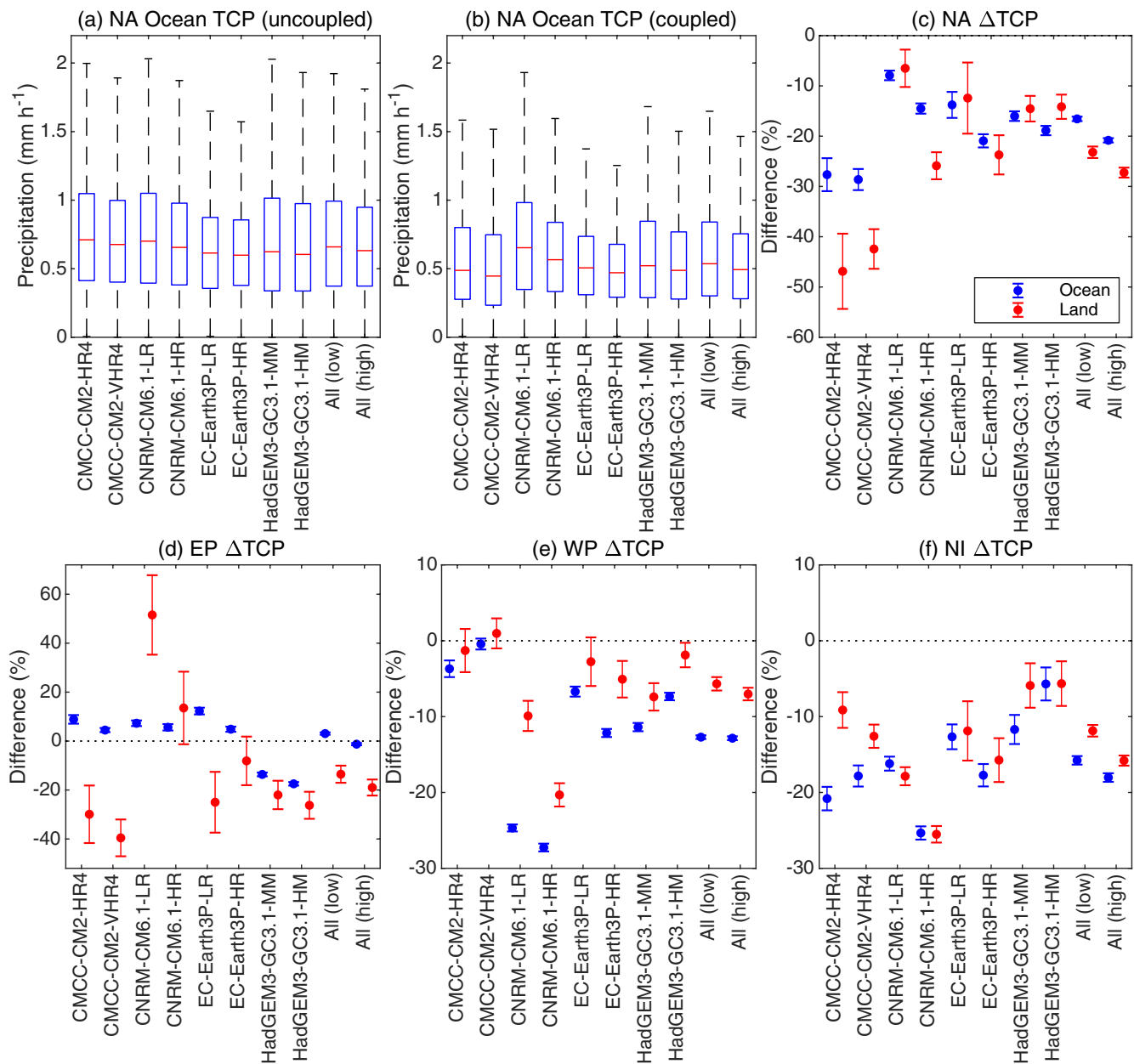
Figure 1. Boxplots of simulated tropical cyclone precipitation (TCP, mm h⁻¹) from 1950–2014 in the (a) uncoupled and (b) coupled simulations by model, and their percentage difference ((coupled minus uncoupled)/ uncoupled, denoted as ΔTCP) over the (c) North Atlantic (NA), (d) eastern North Pacific (EP), (e) western North Pacific (WP), and (f) North Indian (NI) basins. While boxplots in (a and b) are based on TCP over ocean, blue and red error bars in (c–f) represent the ΔTCP over ocean and land, respectively. The two rightmost boxes in (a and b) or blue/red bars in (c–f) refer to the ensemble of all low- and high-resolution model simulations, respectively. The 95% confidence interval in (c–f) is estimated from individually bootstrapping the uncoupled and coupled data 200 times and then calculating their percentage differences (in relative to the mean of uncoupled data) and associated bootstrap standard error.

[−1.7%, −0.8%]) in the eastern North Pacific, −12.8 (95% CI: [−13.1%, −12.6%]) in the western North Pacific, and −17.9 (95% CI: [−18.6%, −17.3%]) in the North Indian. The low-resolution AOGCM ensemble yields comparable TCP, except for the eastern North Pacific (+3.1%). We note that the sign of the TCP difference over the eastern North Pacific varies by GCM (Figure 1d). While two AOGCMs (HadGEM3-GC3.1-MM and HadGEM3-GC3.1-HM) simulate 13.6% and 17.5% less TCP, respectively, the other AOGCMs estimate 4.5%–12.3% more TCP, for reasons explained in the following section.

Landfalling TCP is likewise decreased with ocean coupling (Figures 1c–1f). The high (low) resolution AOG-CM ensemble underestimates landfalling TCP relative to the AGCM ensemble by −27.2% (−23.2%) in the North Atlantic, −20.4% (−13.4%) in the eastern North Pacific, −6.9% (−5.5%) in the western North Pacific, and −15.8% (−11.8%) in the North Indian basin. The TCP differences between the AOGCMs and AGCMs are significantly below 0 at the 0.05 level. Only one AOGCM (CNRM-CM6.1-LR) simulates significantly higher landfalling TCP (+51.5%) over the eastern North Pacific basin (Figure 1d). However, the TCP difference simulated by the CNRM-CM6.1-HR model is not significantly different from 0 (95% CI: [−1.5%, 28.5%]), implying some uncertainty due to model resolution. Furthermore, the impacts of ocean coupling on simulated TCP over the Southern Hemisphere (Figures S6 and S7 in Supporting Information S1) are consistent with those in the Northern Hemisphere, demonstrating the robustness of the finding.

3.3. The Role of Large-Scale SST Biases and TC–Ocean Feedbacks in Modulating TC Precipitation

Figure 2a shows that large-scale SST biases of the AOGCMs (Figure S1 in Supporting Information S1) are critical drivers of the differences in TCP between the coupled and uncoupled simulations. Here we characterized large-scale SST biases as the SST differences between the AOGCMs and prescribed-SSTs AGCMs (i.e., observations) over tropical oceans (5°–30°N). SST biases are generally cold over the North Atlantic and North Indian oceans, ranging from −0.92°C to −0.04°C and −1.13° to 0.1°C, respectively. In contrast, SST biases are mostly warm over the eastern North Pacific (except for the HadGEM3-GC3.1-MM and HadGEM3-GC3.1-HM models) and more mixed in the western North Pacific. These large-scale SST biases significantly influence the TCP differences between the AOGCMs and AGCMs (Figure 2a). Their linear regression suggests that every 1°C of large-scale SST bias increases TCP by 9 ± 0.3% in the AOGCMs relative to the AGCMs. Interestingly, AOGCMs and AGCMs with the same large-scale SST (i.e., zero bias in the AOGCM) produce TCP that differs by −8.2 ± 0.2%. This indicates the importance of some additional mechanism for TCP, potentially local-scale coupling and TC cold wakes.

Therefore, to investigate the potential influence of local-scale SST on TCP, we pose the question: Given the same local SSTs (averaged within a 200 km radius of each TC center) in the AOGCMs and AGCMs, do AOGCMs tend to simulate weaker TCP than AGCMs? By comparing TCP with the same underlying SST, we attempt to evaluate the influence of local-scale SST when controlling for the existence of large-scale SST biases. Figures 2c–2f show ocean TCP differences against pre-TC SSTs in the AOGCMs and AGCMs. Here the pre-TC (3–10 days before TC passage) SSTs are used in order to minimize the impact of TC–ocean interactions on subsequent TCP in the AOGCMs. We confirm the AOGCMs usually produce lower TCP than their corresponding AGCMs over warm ocean water (SST > 26.5°C, a critical SST threshold for TC development in the current climate; Tory & Dare, 2015). The reduced TCP in the AOGCMs relative to AGCMs is evident in a vast majority of the models (high- and low-resolutions included), SST ranges, and ocean basins. We caution that the magnitudes of TCP reduction differ by TC basin, as shown in Figures 2c–2f. Over part of the North Indian Ocean where SSTs are below 27.5°C, there are large positive TCP differences in the HadGEM3-GC3.1-MM and HadGEM3-GC3.1-HM models, because TCP in their AGCM simulations is much lower than those in the AOGCM runs (Figure 2f). But the TCP differences become negative with warmer water (>27.5°C), in line with other GCMs and basins.

Given absent large-scale SST bias and similar local pre-TC SSTs, what physical processes in the AOGCMs may be responsible for the weaker TCP compared to AGCMs? Past studies have linked TC-induced cold wakes to suppressed TC intensity and reduced post-TC precipitation (Karnauskas et al., 2021; Ma et al., 2020). By contrasting SST changes before and after TC passage in both the AOGCMs and AGCMs, we evaluated the impacts of TC cold wakes on TCP and TC intensity. Figures 2b and S8 in Supporting Information S1 show that TCs in the AOGCMs do produce appreciable cold wakes, regardless of large-scale SST biases. The magnitudes of cold wakes (1–4 days after TC passage) are averaged at −0.63° to −0.23°C among all ocean basins and AOGCMs. The more intense TCs tend to produce stronger cold wakes (not shown). We note the magnitudes of simulated cold wakes are smaller than those in observations (−1°C; Vincent, Lengaigne, Madec, et al., 2012), because the GCMs tend to generate weaker TCs than observations (Roberts et al., 2020a). As expected, TCs in the AGCMs do not generate cold wakes (not shown), since SSTs are prescribed from observations as per the HighResMIP protocol (Haarsma et al., 2016). In other words, the
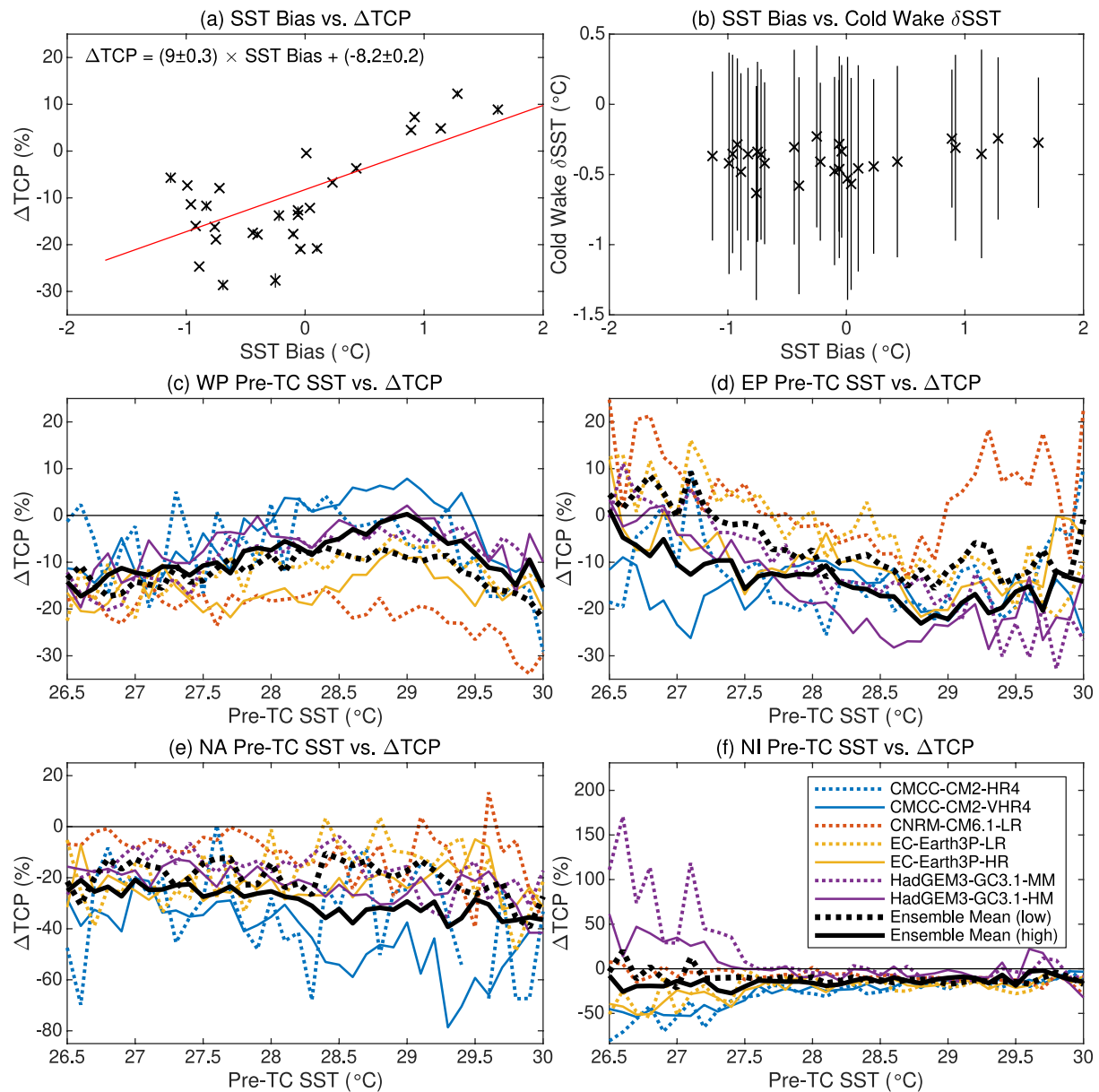
Figure 2. (a) Basin-scale sea surface temperature (SST) bias (°C) averaged over tropical oceans (5°–30°N) from the AOGCM and the percentage difference in ocean tropical cyclone (TC) precipitation (ΔTCP) between the coupled and uncoupled simulations during the period from May–November 1950–2014. (b) Basin-scale SST bias and TC cold wake δSST (°C) in the coupled simulations. (c–f) Ocean-specific ΔTCP with the same pre-TC SST (binned by 0.1°C increment) in the coupled and uncoupled simulations. Each point in (a and b) is derived from a unique combination of four ocean basins and seven climate models (SST data is not available in the CNRM-CM6.1-HR model), with the error bar in y-axis representing its uncertainty range (mean ± one standard deviation).

AOGCMs reproduce active atmosphere–ocean interactions which result in local and negative SST feedback to TCs via cold wakes, but the AGCMs do not. The interactions and feedback have been found to modulate enthalpy flux and regional atmospheric circulation, and therefore negatively affect TC intensity and precipitation (Karnauskas et al., 2021; Kushnir et al., 2002; Ma et al., 2020; Trenberth et al., 1998; Vincent, Lengaigne, Vialard, et al., 2012; Zarzycki, 2016). We find generally decreased TCP in the AOGCMs, in the absence of large-scale SST bias and with similar local pre-TC SSTs. This is in agreement with previous studies on TC-related precipitation (Hasegawa & Emori, 2007; Ma et al., 2020) and can be explained by the thermal feedback of cold wakes, primarily the pressure adjustment mechanism (Pasquero et al., 2021; Renault et al., 2019). Our findings suggest that cold wakes may play an important role in decreasing TCP, independent of the contributions from large-scale SST biases.
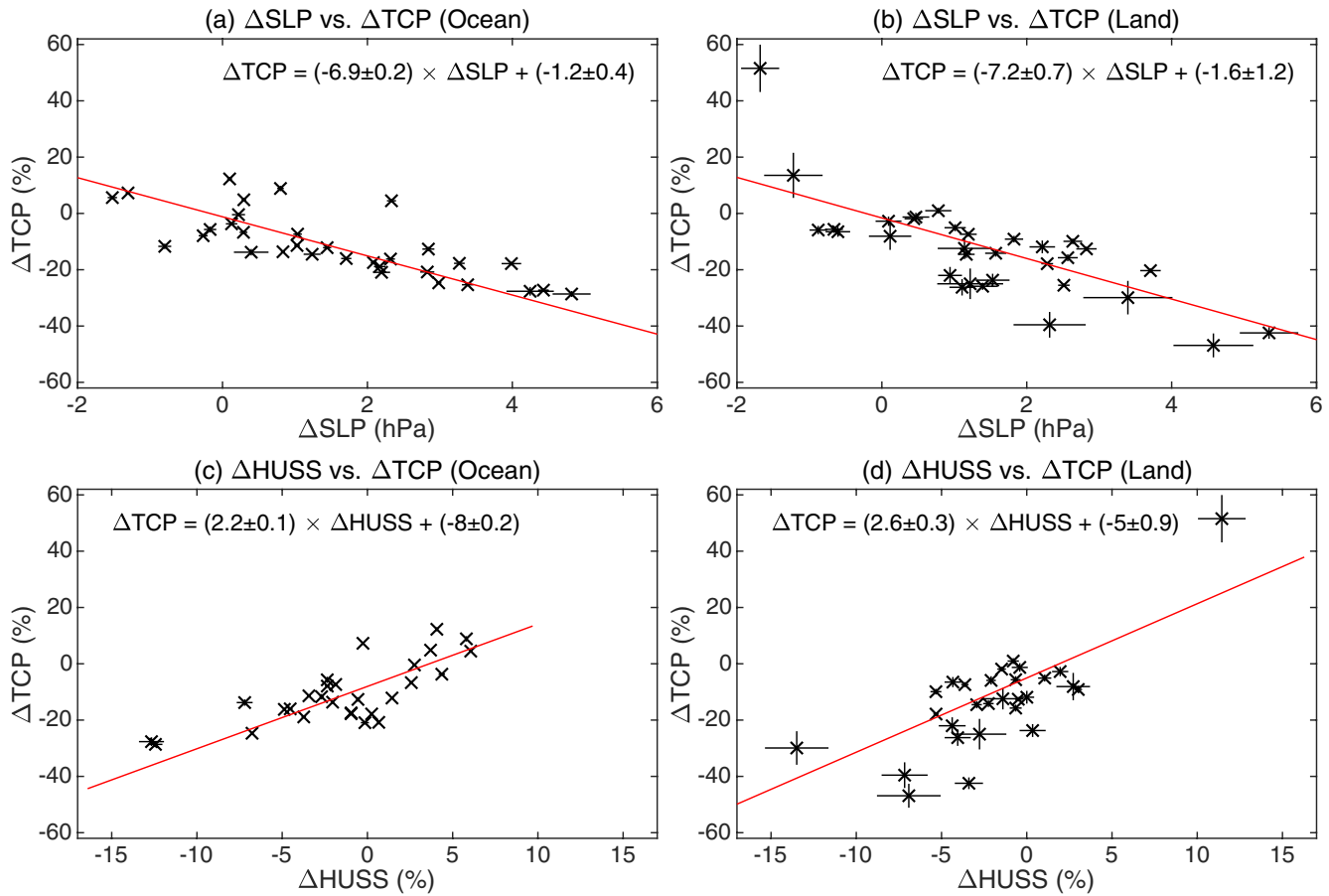
Figure 3. Differences in TC minimum sea level pressure (ΔSLP, hPa), near-surface specific humidity (ΔHUSS, %), and tropical cyclone precipitation (ΔTCP, %) between the coupled and uncoupled simulations over ocean (a and c) and land (b and d). Each point is derived from a unique combination of four ocean basins and seven/eight climate models (ΔHUSS data is not available in the CNRM-CM6.1-HR model), with the error bar representing its uncertainty range (mean ± one standard deviation).

Large-scale SST biases and TC cold wakes, both tied to ocean coupling in the AOGCMs, influence TCP in association with changes in sea level pressure and specific humidity. Figure 3 compares the difference between AOGCM and AGCM TC minimum sea level pressure and near-surface specific humidity. We discover that TC minimum sea level pressure over both ocean and land is typically higher in the AOGCMs compared to AGCMs (Figures 3a and 3b), which means weaker TC intensity. Specific humidity is lower in most AOGCMs (Figures 3c and 3d). Furthermore, both sea level pressure and specific humidity are linearly correlated ($p < 0.01$) with the difference in TCP.

3.4. Projected Tropical Cyclone Precipitation and Its Dependence on Ocean Coupling

The AOGCMs and AGCMs consistently predict an increase in ocean TCP during 2015–2050 relative to 1950–2014 across all TC basins (Figure 4). The high-resolution AGCM (AOGCM) ensemble projects TCP to increase by 3.7% (10.9%) in the North Atlantic, 5.0% (6.5%) in the eastern North Pacific, 1.8% (4.4%) in the western North Pacific, and 3.0% (0.2%) in the North Indian oceans. The increases in ocean TCP are significant at 0.05 level, because their 95% CIs are generally above 0 (except for the AOGCMs runs in the North Indian Ocean). The low-resolution GCMs produce similar changes, despite intermodel differences in their magnitudes.

Landfalling TCP is expected to increase in the North Atlantic and western North Pacific basins, whereas TCP changes in the eastern North Pacific and North Indian basins are mixed (Figure 4). The high-resolution AGCM (AOGCM) ensemble predicts landfalling TCP to rise by 4.2% (4.5%) and 8.3% (5.0%) over the
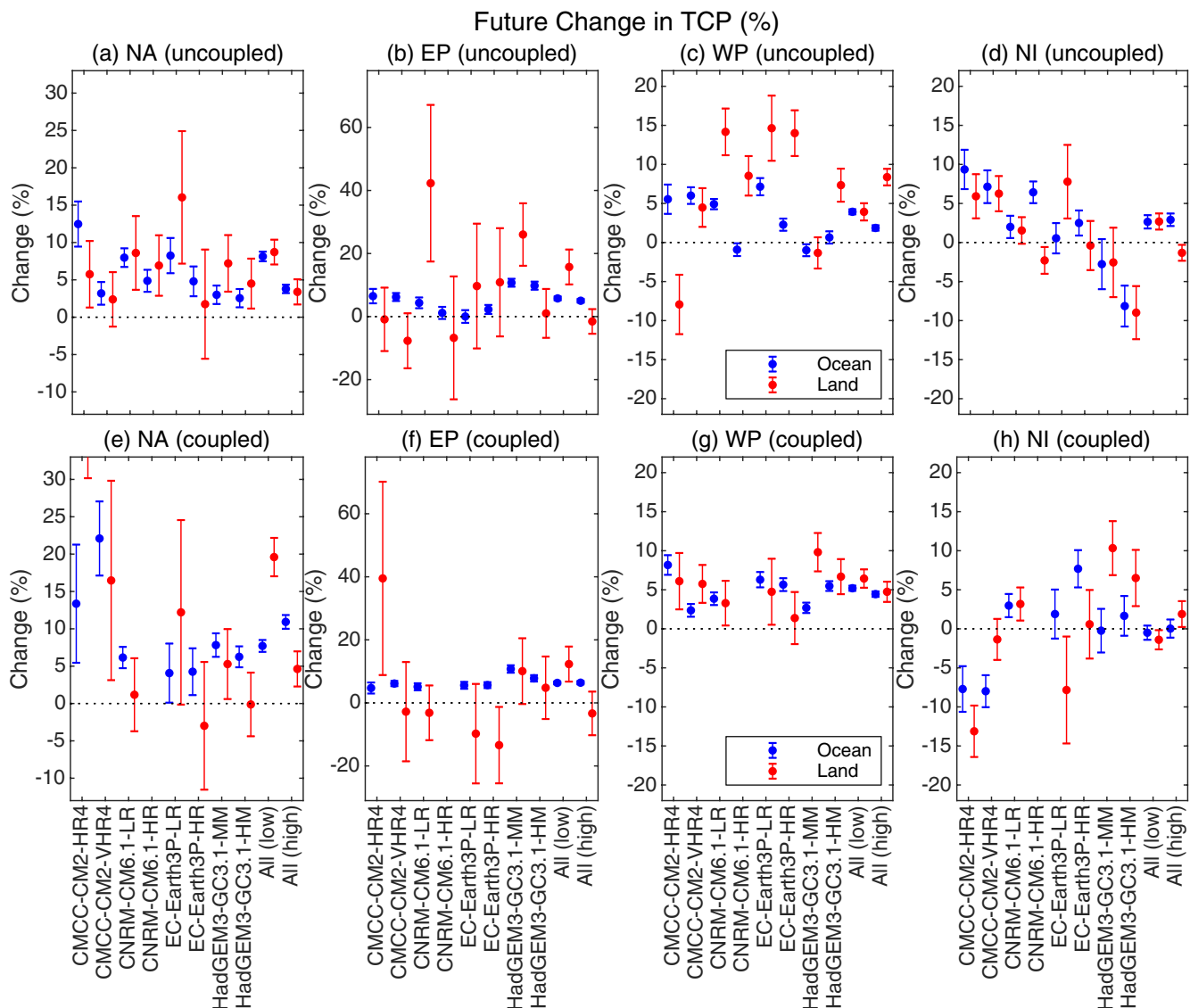
Figure 4. Percentage changes in 2015–2050 tropical cyclone precipitation (TCP) relative to 1950–2014 by model and basin in the (a–d) uncoupled and (e–h) coupled simulations. Blue and red error bars in each panel represent future changes in TCP over ocean and land, respectively. The basins include the North Atlantic (NA), eastern North Pacific (EP), western North Pacific (WP), and North Indian (NI). The two rightmost blue/red bars in each panel refer to the ensemble of all low- and high-resolution model simulations, respectively. The 95% confidence interval is estimated from individually bootstrapping the 2015–2050 and 1950–2014 data 200 times and then calculating their percentage differences (in relative to the mean of 1950–2014 data) and associated bootstrap standard error. The first red error bar in (e) extends beyond the figure because of its large uncertainty in future TCP change.

North Atlantic and western North Pacific basins, respectively. These increases are significant at the 0.05 level, as are the changes simulated by the low-resolution GCMs. In the eastern North Pacific, however, landfalling TCP is projected to decrease by 1.7% (1.9%) in the high-resolution AGCM (AOGCM) ensemble, although the changes are insignificant. Conversely, the low-resolution AGCM (AOGCM) ensemble estimates a substantial TCP intensification of 16.9% (11.4%). Over the North Indian basin, landfalling TCP is expected to decrease (increase) significantly by 1.2% (2.3%) in the high-resolution AGCMs (AOGCMs). The low-resolution AGCMs and AOGCMs yield changes of 2.7% and −1.2%, respectively. The opposite changes demonstrate a large uncertainty in landfalling TCP predictions over the eastern North Pacific and North Indian basins. In summary, future TCP over land and ocean is generally predicted to increase, with a few exceptions for individual GCMs and basins. The magnitude of the TCP changes can vary by a factor of three depending on whether the ocean is coupled with the atmosphere, for example for North Atlantic TCs over ocean in the high-resolution simulations. What is more, the predicted increase in TCP is robust over the

Southern Hemisphere (Figures S9 and S10 in Supporting Information S1). Our findings align with Knutson et al. (2020), Scoccimarro et al. (2014), and Patricola and Wehner (2018) who discovered robust increases in TCP with future anthropogenic warming.

4. Conclusions

This study aims to quantify the impacts of ocean coupling—associated with basin-scale SST biases and local-scale TC–ocean feedbacks—on simulated and projected TCP. We find that both the AGCMs and AOG-CMs mostly underestimate TCP as compared to the TRMM observations (except in the eastern North Pacific). Ocean coupling generally leads to decreased TCP during 1950–2014 over ocean and land. The TCP decrease exhibits a low sensitivity to model resolution across TC basins. Large-scale SST biases in the AOG-CMs are critical drivers of the TCP difference. Every 1°C of large-scale SST cold bias decreases TCP by $9 \pm 0.3\%$ in the AOGCMs relative to the AGCMs. Moreover, local TC–ocean feedbacks via SST cold wakes also play an important role in decreasing TCP in the AOGCMs, as demonstrated by the TCP decline with the absence of large-scale SST biases. Both large-scale SST biases and cold wakes are present due to ocean coupling in the AOGCMs. Altogether the two features influence TCP by modulating its sea level pressure and specific humidity, with decreased TCP in the AOGCMs associated with higher sea level pressure (i.e., weaker TC intensity) and lower humidity. Given the design of the HighResMIP AGCM and AOGCM experiments, it is very difficult to completely isolate the effects of large-scale SST biases and cold wakes on the processes and therefore TCP. A better understanding of their individual effects warrants a further study, such as running AGCM-like experiments with TC cold wakes specified (Karnauskas et al., 2021) or mechanistic experiments based on specific TC events using a simple ocean model that lacks basin-scale SST biases, as suggested by Patricola and Wehner (2018).

During the future period of 2015–2050, TCP over ocean is projected to increase across all TC basins, consistent in the AOGCMs and AGCMs, although the magnitude can vary by up to a factor of three depending on whether the ocean is coupled. Landfalling TCP will likewise increase in the North Atlantic and western North Pacific basins, but TCP changes over the eastern North Pacific and North Indian basins are mixed. Our findings highlight the importance of better understanding and characterizing the physical mechanisms governing the accurate representations of SSTs, TCs, and TCP. Bridging the gap between AOGCMs and AGCMs may provide a better constraint on future TCP projections, and therefore a more robust assessment of future climate change risk.

Conflict of Interest

There is no financial conflict of interest for any author.

Data Availability Statement

The climate data sets and tropical cyclone (TC) tracks used in this work are publicly available, with their DOIs/links cited in this manuscript. The HighResMIP–PRIMAVERA climate model outputs are available on the Earth System Grid Federation nodes (https://esgf-index1.ceda.ac.uk/search/cmip6-ceda) under references Scoccimarro et al. (2017a, 2017b), Voldoire (2019a, 2019b), EC-Earth Consortium (2019a, 2019b), and Roberts (2017a, 2017b). The model data can also be accessed at the UK Centre for Environmental Data Analysis's JASMIN platform (https://www.ceda.ac.uk/services/jasmin/). Simulated TC tracks can be accessed through the UK Centre for Environmental Data Analysis under references Roberts (2019a, 2019b). Observed TC tracks in the North Atlantic and eastern North Pacific basins are obtained from NOAA National Hurricane Center (https://www.nhc.noaa.gov/data/#hurdat). Observed TC tracks in the western North Pacific and North Indian basins are obtained from the U.S. Navy's Joint Typhoon Warning Center (https://www.metoc.navy.mil/jtwc/jtwc.html?best-tracks). The Tropical Rainfall Measuring Mission (TRMM) data set is accessed from NASA's Goddard Earth Sciences Data and Information Services Center (https://doi.org/10.5067/TRMM/TMPA/3H/7).

References

Bador, M., Boé, J., Terray, L., Alexander, L. V., Baker, A., Bellucci, A., et al. (2020). Impact of higher spatial atmospheric resolution on precipitation extremes over land in global climate models. *Journal of Geophysical Research: Atmospheres*, *125*. https://doi.org/10.1029/2019jd032184

Bakkensen, L. A., Park, D. S. R., & Sarkar, R. S. R. (2018). Climate costs of tropical cyclone losses also depend on rain. *Environmental Research Letters*, *13*(7), 074034. https://doi.org/10.1088/1748-9326/aad056

Bell, J. E., Brown, C. L., Conlon, K., Herring, S., Kunkel, K. E., Lawrimore, J., et al. (2018). Changes in extreme events and the potential impacts on human health. *Journal of the Air & Waste Management Association*, *68*(4), 265–287. https://doi.org/10.1080/10962247.2017.1401017

Centre for Research on the Epidemiology of Disasters (CRED). (2021). *EM-DAT | The international disasters database*. Retrieved From https://www.emdat.be/

Cherchi, A., Fogli, P. G., Lovato, T., Peano, D., Iovino, D., Gualdi, S., et al. (2019). Global mean climate and main patterns of variability in the CMCC-CM2 coupled model. *Journal of Advances in Modeling Earth Systems*, *11*(1). https://doi.org/10.1029/2018MS001369

Chu, J. H., Sampson, C. R., Levine, A. S., & Fakuda, E. (2002). *The Joint Typhoon Warning Center tropical cyclone best-tracks, 1945–2000*. Retrieved From https://www.metoc.navy.mil/jtwc/products/best-tracks/tc-bt-report.html

EC-Earth Consortium. (2019a). *EC-Earth-Consortium EC-Earth3P-HR model output prepared for CMIP6 HighResMIP*. https://doi.org/10.22033/ESGF/CMIP6.2323

EC-Earth Consortium. (2019b). *EC-Earth-Consortium EC-Earth3P model output prepared for CMIP6 HighResMIP*. https://doi.org/10.22033/ESGF/CMIP6.2322

Haarsma, R., Acosta, M., Bakhshi, R., Bretonnière, P. A., Caron, L. P., Castrillo, M., et al. (2020). HighResMIP versions of EC-Earth: EC-Earth3P and EC-Earth3P-HR—Description, model computational performance and basic validation. *Geoscientific Model Development*, *13*(8), 3507–3527. https://doi.org/10.5194/gmd-13-3507-2020

Haarsma, R. J., Roberts, M. J., Vidale, P. L., Catherine, A., Bellucci, A., Bao, Q., et al. (2016). High Resolution Model Intercomparison Project (HighResMIP v1.0) for CMIP6. *Geoscientific Model Development*, *9*,4185–4208. https://doi.org/10.5194/gmd-9-4185-2016

Hasegawa, A., & Emori, S. (2007). Effect of air-sea coupling in the assessment of CO_2-induced intensification of tropical cyclone activity. *Geophysical Research Letters*, *34*. https://doi.org/10.1029/2006GL028275

Hodges, K., Cobb, A., & Vidale, P. L. (2017). How well are tropical cyclones represented in reanalysis datasets? *Journal of Climate*, *30*, 5243–5264. https://doi.org/10.1175/JCLI-D-16-0557.1

Hsu, W. C., Patricola, C. M., & Chang, P. (2019). The impact of climate model sea surface temperature biases on tropical cyclone simulations. *Climate Dynamics*, *53*(1–2), 173–192. https://doi.org/10.1007/s00382-018-4577-5

Huffman, G. J., Adler, R. F., Bolvin, D. T., Gu, G., Nelkin, E. J., Bowman, K. P., et al. (2007). The TRMM Multisatellite Precipitation Analysis (TMPA): Quasi-global, multiyear, combined-sensor precipitation estimates at fine scales. *Journal of Hydrometeorology*, *8*, 38–55. https://doi.org/10.1175/JHM560.1

Karnauskas, K. B., Zhang, L., & Emanuel, K. A. (2021). The feedback of cold wakes on tropical cyclones. *Geophysical Research Letters*, *48*(7), e2020GL091676. https://doi.org/10.1029/2020GL091676

Knutson, T., Camargo, S. J., Chan, J. C. L., Emanuel, K., Ho, C. H., Kossin, J., et al. (2020). Tropical cyclones and climate change assessment part II: Projected response to anthropogenic warming. *Bulletin of the American Meteorological Society*, *101*(3), E303–E322. https://doi.org/10.1175/BAMS-D-18-0194.1

Kushnir, Y., Robinson, W. A., Bladé, I., Hall, N. M. J., Peng, S., & Sutton, R. (2002). Atmospheric GCM response to extratropical SST anomalies: Synthesis and evaluation. *Journal of Climate*, *15*(16), 2233–2256. https://doi.org/10.1175/1520-0442(2002)015<2233:AGRTES>2.0.CO;2

Landsea, C. W., & Franklin, J. L. (2013). Atlantic hurricane database uncertainty and presentation of a new database format. *Monthly Weather Review*, *141*(10), 3576–3592. https://doi.org/10.1175/MWR-D-12-00254.1

Li, H., & Sriver, R. L. (2018). Tropical cyclone activity in the high-resolution Community Earth System Model and the impact of ocean coupling. *Journal of Advances in Modeling Earth Systems*, *10*, 165–186. https://doi.org/10.1002/2017MS001199

Li, H., & Sriver, R. L. (2019). Impact of air–sea coupling on the simulated global tropical cyclone activity in the high-resolution Community Earth System Model (CESM). *Climate Dynamics*, *53*, 3731–3750. https://doi.org/10.1007/s00382-019-04739-8

Liu, J., Curry, J. A., Clayson, C. A., & Bourassa, M. A. (2011). High-resolution satellite surface latent heat fluxes in North Atlantic hurricanes. *Monthly Weather Review*, *139*(9), 2735–2747. https://doi.org/10.1175/2011MWR3548.1

Ma, Z., Fei, J., Lin, Y., & Huang, X. (2020). Modulation of clouds and rainfall by tropical cyclone's cold wakes. *Geophysical Research Letters*, *47*(17), e2020GL088873. https://doi.org/10.1029/2020GL088873

Mendelsohn, R., Emanuel, K., Chonabayashi, S., & Bakkensen, L. (2012). The impact of climate change on global tropical cyclone damage. *Nature Climate Change*, *2*(3), 205–209. https://doi.org/10.1038/nclimate1357

NOAA National Centers for Environmental Information. (2021). *Billion-dollar weather and climate disasters: Overview | National Centers for Environmental Information (NCEI)*. Retrieved From https://www.ncdc.noaa.gov/billions/

Pasquero, C., Desbiolles, F., & Meroni, A. N. (2021). Air-sea interactions in the cold wakes of tropical cyclones. *Geophysical Research Letters*, *48*(2), e2020GL091185. https://doi.org/10.1029/2020GL091185

Patricola, C. M., & Wehner, M. F. (2018). Anthropogenic influences on major tropical cyclone events. *Nature*, *563*(7731), 339–346. https://doi.org/10.1038/s41586-018-0673-2

Price, J. F. (1981). *Upper ocean response to a hurricane*. Woods Hole Oceanographic Institution. https://doi.org/10.1575/1912/10271

Rappaport, E. N. (2014). Fatalities in the united states from Atlantic tropical cyclones: New data and interpretation. *Bulletin of the American Meteorological Society*, *95*(3), 341–346. https://doi.org/10.1175/BAMS-D-12-00074.1

Rappaport, E. N., & Blanchard, B. W. (2016). Fatalities in the United States indirectly associated with Atlantic tropical cyclones. *Bulletin of the American Meteorological Society*, *97*, 1139–1148. https://doi.org/10.1175/BAMS-D-15-00042.1

Renault, L., Masson, S., Oerder, V., Jullien, S., & Colas, F. (2019). Disentangling the mesoscale ocean-atmosphere interactions. *Journal of Geophysical Research: Oceans*, *124*(3), 2164–2178. https://doi.org/10.1029/2018JC014628

Richter, I. (2015). Climate model biases in the eastern tropical oceans: Causes, impacts and ways forward. *Wiley Interdisciplinary Reviews: Climate Change*, *6*(3), 345–358. https://doi.org/10.1002/wcc.338

Richter, I., & Tokinaga, H. (2020). An overview of the performance of CMIP6 models in the tropical Atlantic: Mean state, variability, and remote impacts. *Climate Dynamics*, *55*(9–10), 2579–2601. https://doi.org/10.1007/s00382-020-05409-w

References From the Supporting Information

Eyring, V., Bony, S., Meehl, G. A., Senior, C. A., Stevens, B., Stouffer, R. J., & Taylor, K. E. (2016). Overview of the Coupled Model Inter-comparison Project Phase 6 (CMIP6) experimental design and organization. *Geoscientific Model Development*, *9*(5), 1937–1958. https://doi.org/10.5194/gmd-9-1937-2016

Kennedy, J., Titchner, H., Rayner, N., & Roberts, M. (2017). *Input4MIPs.MOHC.SSTsAndSeaIce.HighResMIP.MOHC-HadISST-2-2-0-0-0*. https://doi.org/10.22033/ESGF/input4MIPs.1221

O'Neill, B. C., Tebaldi, C., Van Vuuren, D. P., Eyring, V., Friedlingstein, P., Hurtt, G., et al. (2016). The Scenario Model Intercomparison Project (ScenarioMIP) for CMIP6. *Geoscientific Model Development*, *9*(9), 3461–3482. https://doi.org/10.5194/gmd-9-3461-2016

Poli, P., Hersbach, H., Dee, D. P., Berrisford, P., Simmons, A. J., Vitart, F., et al. (2016). ERA-20C: An atmospheric reanalysis of the twentieth century. *Journal of Climate*, *29*(11), 4083–4097. https://doi.org/10.1175/JCLI-D-15-0556.1